Electronic Supplementary Material (ESI) for ChemComm.

Supporting Information

Cobalt Amine Complexes and Ru265 Inhibit Mitochondrial Calcium Uptake Through Interactions with the DIME Region of the Mitochondrial Calcium Uniporter Pore

Joshua J. Woods,[a,b] Madison X. Rodriguez,[c] Chen-Wei Tsai,[c] Ming-Feng Tsai,[c] and Justin J. Wilson[a]*

[a]Department of Chemistry and Chemical Biology, Cornell University, Ithaca, NY, USA
[b]Robert F. Smith School for Chemical and Biomolecular Engineering, Cornell University, Ithaca, NY, USA
[c]Department of Physiology and Biophysics, University of Colorado Anschutz Medical Campus, Aurora, CO, USA

*Corresponding author: jjw275@cornell.edu

TABLE OF CONTENTS

page

LIST OF TABLES S3

LIST OF FIGURES S4

1. GENERAL S6

2. MITOCHONDRIAL CALCIUM UPTAKE STUDIES S6

3. CYTOTOXICITY AND CELLULAR UPTAKE STUDIES S8

4. DOCKING STUDIES S9

5. SUPPLEMENTARY FIGURES AND TABLES S10

6. REFERENCES S18

LIST OF TABLES

Table page

Table S1. Comparison of the relative docking scores of the metal complexes docked into the solvent accessible region of the MCU. S18

LIST OF FIGURES

Figure page

Figure S1. Quantification of MCU-inhibitory activity of the Co^{3+} complexes as reflected by mt-Ca^{2+} uptake rate in permeabilized HeLa cells (5×10^6 cells mL^{-1}) at 10 and 50 μM. Data are reported as the mean % inhibition compared to control cells ± 1 standard deviation (SD, *n* = 3). 10

Figure S2. Representative traces of extramitochondrial Ca^{2+} clearance in permeabilized HeLa cells (5×10^6 cells mL^{-1}) treated with either 10 μM or 50 μM of (a) **1**, (b) **2**, (c) **3**, (d) **4**, (e) **5**, or (f) **6**. Arrows indicate addition of 10 μM Ca^{2+}. Each complex was tested in triplicate using independently prepared cell suspensions and complex stock solutions. 10

Figure S3. (a) Representative traces of extramitochondrial Ca^{2+} clearance in permeabilized HeLa cells (5×10^6 cells mL^{-1}) treated with varying concentrations of Ru265 after addition of 10 μM Ca^{2+}. The arrow indicates time of addition. (b) Dose-response curve for mt-Ca^{2+} uptake inhibition by Ru265. Data are represented as mean ± SD (*n* = 3 – 4). 11

Figure S4. (a) Representative traces of extramitochondrial Ca^{2+} clearance after addition of 10 μM Ca^{2+} in permeabilized HeLa cells (5×10^6 cells mL^{-1}) treated with varying concentrations of **1**. The arrow indicates time of Ca^{2+} addition. (b) Dose-response curve for mt-Ca^{2+} uptake inhibition by **1**. Data are represented as mean ± SD (*n* = 3 – 4). 11

Figure S5. (a) Representative traces of extramitochondrial Ca^{2+} clearance after addition of 10 μM Ca^{2+} in permeabilized HeLa cells (5×10^6 cells mL^{-1}) treated with varying concentrations of **3**. The arrow indicates time of Ca^{2+} addition. (b) Dose-response curve for mt-Ca^{2+} uptake inhibition by **3**. Data are represented as mean ± SD (*n* = 3 – 4). 12

Figure S6. (a) Representative traces of extramitochondrial Ca^{2+} clearance after addition of 10 μM Ca^{2+} in permeabilized HeLa cells (5×10^6 cells mL^{-1}) treated with varying concentrations of **6**. The arrow indicates time of Ca^{2+} addition. (b) Dose-response curve for mt-Ca^{2+} uptake inhibition by **6**. Data are represented as mean ± SD (*n* = 3 – 4). 12

Figure S7. Representative traces of extramitochondrial Ca^{2+} clearance after addition of 15 μM Ca^{2+} in permeabilized HEK293 cells (10^7 cells mL^{-1}) treated with different concentrations of (a) **3**, (b) **6**, or (c) Ru265. (d) Dose-response curves for mt-Ca^{2+} uptake inhibition by **3**, **6**, and Ru265. Data are represented as mean ± S.E.M. (*n* = 3 – 5). 12

Figure S8. Representative traces of extramitochondrial Ca^{2+} clearance after addition of 10 μM Ca^{2+} in permeabilized HeLa cells (5×10^6 cells mL^{-1}) treated with varying concentrations of (a) **3a** or (b) **3b**. The arrow indicates time of Ca^{2+} addition. (c) Dose-response curves for mt-Ca^{2+} uptake inhibition by **3a** and **3b**. Data are represented as mean ± SD (*n* = 3 – 4). 13

Figure S9. (a) Representative traces of extramitochondrial Ca^{2+} clearance after addition of 10 μM Ca^{2+} in permeabilized HeLa cells (5×10^6 cells mL^{-1}) treated with 10 μM ethylenediamine (en). The arrow indicates time of Ca^{2+} addition. (b) Dose-response plot for mt-Ca^{2+} uptake in the presence of en. Data are represented as mean ± SD (*n* = 3). 13

Figure S10. Cell viability curves of HeLa and HEK293T cells treated with varying concentrations of (a) **3** and (b) **6** for 72 h. Results are represented as mean ± SD of three independent trials with 6 wells/concentration. 14

Figure S11. Normalized red/green fluorescence intensity of HeLa and HEK293T cells after treatment with the corresponding compounds and 10 μM JC-1 dye. See Figure S12-S13 for representative confocal fluorescence microscopy images. 14

Figure S12. Representative confocal fluorescence microscopy images of HeLa cells treated with JC-1 dye and (a) no compound (b) 50 μM CCCP for 2 min, (c) 50 μM **3** for 24 h, and (d) 50 μM **6** for 24 h. The scale bar represents 20 μm. 14

Figure S13. Representative confocal fluorescence microscopy images of HEK293T cells treated with JC-1 dye and (a) no compound, (b) 50 μM CCCP for 2 min, (c) 50 μM **3** for 24 h, and (d) 50 μM **6** for 24 h. The scale bar represents 20 μm. 15

Figure S14. Cellular accumulation of Ru265, **3**, and **6** in HeLa and HEK293T cells treated with 50 μM complex for 3 h in DMEM supplemented with 10% FBS. Data are represented as mean ± SD (n = 3). 15

Figure S15. (a) Representative mt-Ca^{2+} accumulation after addition of 100 μM histamine in HeLa cells pretreated with 0 or 50 μM of Ru265, **3**, or **6** for 1 h and then loaded with 2 μM Rhod2AM. The arrow indicates time of histamine addition. (b) Quantification of peak F/F_0 at the point indicated by the star in panel a. (c) Representative fluorescence microscopy images of HeLa cells treated as described above at the point labeled by * in panel a. The scale bar represents 10 μm. Data are represented as mean F/F_0 of at least four cells ± SD from two independent biological replicates. **p<0.01 *vs* control, ns = not significant..... 16

Figure S16. Comparison of the cobalt concentration in the extramitochondrial (EM) and mitochondrial (M) fraction of HeLa cells treated with **3**. The cells were treated with 50 μM complex for 3 h with no recovery in drug free medium. Cobalt concentration was normalized to protein content, which was determined using the BCA assay. Data are mean of three trials ± standard devation. n = 3, **p<0.01..... 17

Figure S17. Top-down view of (a) Ru265, (b) **3**, and (c) **6** docked into the human MCU (PBD 6O5B). The surface is colored by amino acid hydrophobicity (lime green = hydrophilic, orange = hydrophobic). 17

1. GENERAL

Reagents and Materials. Cobalt chloride hexahydrate ($CoCl_2 \cdot 6H_2O$) was purchased from Ward's Science (Rochester, NY) and used as received. All other reagents were obtained commercially and used without further purification. Water (18 MΩ·cm) was purified using an ELGA PURELAB flex 2 (High Wycombe, UK).

Physical Measurements. 1D-NMR spectra were acquired at 25 °C on a 500 MHz Bruker AV 3HD spectrometer equipped with a broadband Prodigy cryoprobe (Bruker, Billerica, MA). ^{1}H NMR spectra in D_2O were referenced to dioxane (0.1 %) as an internal standard (3.75 ppm vs tetramethylsilane at 0 ppm). UV-vis spectra were acquired using a Shimadzu UV-1900 spectrophotometer (Shimadzu, Kyoto, Japan) fitted with a temperature-controlled circulating water bath. Elemental analyses (C, H, N) were carried out by Atlantic Microlab Inc. (Norcross, GA). Fluorescence and absorbance of samples in 96 well plates were measured using a BioTek Synergy HT plate reader (Winooski, VT). Graphite furnace atomic absorption spectroscopy (GFAAS) was performed using a PinAAcle 900Z spectrometer (Perkin Elmer, Waltham, MA). Standardized solutions (0–100 µg/L) of cobalt were used for calibration. The concentration of all cobalt stock solutions was checked by GFAAS or UV/vis spectroscopy using the known extinction coefficients of the complexes. High performance liquid chromatography (HPLC) was performed using a LC-20AT pump with a SPD-20AV UV/vis detector monitored at 270 nm (Shimadzu, Kyoto, Japan) using an Ultra Aqueous C18 column (100 Å; 5 µM; 250 mm × 4.6 mm; Restek, Bellefonte) and an isocratic elution of H_2O with 1% MeOH and 0.1% trifluoroacetic acid at a flow rate of 1 mL/min. Statistical analyses were performed using GraphPad Prism 7.0 software by applying a non-paired student's t-test.

Synthesis. The compounds Ru265,[1] Ru360′,[2] $[Co(NH_3)_6]Cl_3$, $[Co(NH_3)_5Cl]Cl_2$,[3] rac-$[Co(en)_3]Cl_3$,[4] (Λ)-$[Co(en)_3]Cl_3$,[5] (Δ)-$[Co(en)_3]Cl_3$,[5] $[Co(dien)_2]Cl_3$,[6] $[Co(tacn)_2]Cl_3$,[7] and $[Co(sep)]^{3+}$,[8] were all synthesized by literature procedures. Characterization data matched literature reported values.

Cell Lines and Culture Conditions. HeLa and HEK293T cells were obtained from American Type Culture Collection (ATCC, Washington DC) and cultured as adherent monolayers in a humidified atmosphere containing 5% CO_2 in Dulbecco's Modified Eagle's Medium (DMEM) containing 4.5 g/L glucose, L-glutamine, and 3.7 sodium bicarbonate supplemented with 10% fetal bovine serum (FBS) and 100 U/mL penicillin/streptomycin (Corning Life Sciences, Tewksbury, MA). All cell lines were checked for contamination monthly using the PlasmoTest mycoplasma detection kit from InvivoGen (San Diego, CA). All reagents and solutions used in biological studies were sterile filtered through a 0.2 µm filter and maintained under sterile conditions.

2. MITOCHONDRIAL CALCIUM UPTAKE STUDIES

Mitochondrial Ca^{2+} Uptake in Permeabilized HeLa Cells. HeLa cells were grown to near confluency in a 10 cm^2 dish and harvested using 0.05% trypsin + 0.53 mM ethylenediaminetetraacetic acid (EDTA; Corning Life Sciences). The cells were pelleted by centrifugation and suspended in cold phosphate buffered saline (PBS, Corning Life Sciences) supplemented with 5 mM EDTA (pH 7.4) and counted using trypan blue. The remaining cells were pelleted by centrifugation at 800 × *g* for 5 minutes and resuspended in ice cold high KCl solution (125 mM KCl, 20 mM HEPES, 2 mM K_2HPO_4, 5 mM glutamate, 5 mM malate, 1 mM MgCl2, pH 7.2 with KOH) supplemented with 80 µM digitonin and 1 µM thapsigargin. The final solution contained <0.1% DMSO, originating from the digitonin and thapsigargin stocks. The cells were incubated on ice for 15 min and centrifuged at 200 × *g* for 10 min at 4 °C. The pelleted cells were then resuspended in high KCl solution containing 1 µM Calcium Green 5N (ThermoFisher, Waltham, MA) and 2 mM succinate to a final density of 5×10^6 cells/mL. For each experiment, 100 µL of the cell suspension was placed in each

well of a black-walled 96 well plate, treated with the desired concentration of the test complex, and allowed to equilibrate at room temperature for ~200 s. The background fluorescence of each well was recorded for 60 s prior to addition of 10 μM $CaCl_2$. The change in fluorescence of the dye (ex. 488 / em. 528) in response to Ca^{2+} was recorded every 5 s for at least 120 s or until the fluorescence returned to the baseline. The mitochondrial Ca^{2+} uptake rate was calculated as the slope of the linear fit of the first 25 s of the fluorescence response. Control cells that were not treated with compound were handled identically to the treated cells to account for different incubation lengths. The Ca^{2+} uptake rate of treated cells was normalized to that of the controls cells (0% inhibition) and each replicate was performed using independently prepared cells suspensions to account for differences in cell count. Additionally, each replicate was performed using an independently prepared stock solution of complex from an independently synthesized batch of compound to account for potential differences in synthetic preparations (n = 3 – 5).

Mitochondrial Ca^{2+} Uptake in Intact HeLa Cells using Rhod2AM. Approximately 1 × 10^5 HeLa cells were seeded in 35 mm glass-bottomed dishes (MatTek Life Sciences, Ashland, MA) and incubated overnight at 37 °C. The following day, cells were treated with the desired metal complex (50 μM) in DMEM supplemented with 10% FBS for 1 h at 37 °C. The culture media was removed, and the cells were washed with 1 × 1 mL phosphate buffered saline (PBS, Corning Life Sciences) before the cells were incubated in extracellular medium (ECM; 135 mM NaCl, 20 mM HEPES, 5 mM KCl, 1 mM $MgCl_2$, 1 mM $CaCl_2$) supplemented with 10 mM glucose, 3.2 mg/mL bovine serum albumin (BSA), 0.003% pluronic F127, and 2 μM Rhod2AM (Molecular Probes) in the dark for 30 min at room temperature. The ECM was then removed, the cells were washed with 1 × 1 mL ECM, and the cells were treated with fresh ECM supplemented with 10 mM glucose and 3.2 mg/mL BSA and incubated for a further 30 min in the dark at room temperature. The buffer was then removed, and the cells washed with 1 × 1 mL ECM and treated with ECM supplemented with 10 mM glucose and 3.2 mg/mL BSA at 37 °C for 15 min before imaging using a Zeiss LSM i880 confocal fluorescence microscope using a 40× oil objective with an excitation of 561 nm and an emission window of 568 – 712 nm. After ~ 30 s of baseline recording, histamine (100 μM) was added to the dish and fluorescence images were recorded every 3 s to monitor mt-Ca^{2+} uptake. Images were analyzed and quantified using ImageJ (NIH) and the corrected total cellular fluorescence (CTCF) was calculated using the following formula:

CTCF = Integrated density – (area of cell × mean fluorescence of background reading)

The average of at least four individual cells was used to determine the average CTCF for reach replicate. Results are reported as the average of two independent biological replicates ± SD.

Mitochondrial Ca^{2+} Uptake in Permeabilized HEK Cells. WT or MCU-KO HEK293T cells were cultured in 10-cm dishes. Transient expression using Lipofectamine 3000 (Life Technologies) was performed when the cell confluency reached 60-70%. Two days after transfection, cells were suspended in a wash buffer (120 mM KCl, 25 mM HEPES, 2 mM KH_2PO_4, 1 mM $MgCl_2$, 50 μM EGTA, pH 7.2-KOH), pelleted at 1,200 g for 2 min, and then resuspended in a recording buffer (120 mM KCl, 25 mM HEPES, 2 mM KH_2PO_4, 1 mM $MgCl_2$, 5 mM succinate, pH 7.2-KOH) to 10^7 cells/mL. 2 mL of cell suspension was placed into a stirred quartz cuvette in a Hitachi F-7100 spectrofluorometer (ex: 506 nm; em: 532 nm). The recording temperature was controlled at 25 ℃. 0.5 μM calcium green 5N (Life Technologies) was added, followed by 30 μM digitonin (Sigma, D141). MCU inhibitor was added before or shortly after adding 15 μM $CaCl_2$. 100 nM Ru360 was used to completely inhibit mitochondrial Ca^{2+} uptake. The % inhibition of the uniporter treated with various compounds at various concentrations was reported as $(S - S_{In})/(S-S_{Ru})$, where S is the slope of the fluorescence signal reduction after Ca^{2+} addition, S_{In} is the slope of signal reduction in the presence of an indicated inhibitor, and S_{Ru} is the slope of the fluorescence signal after adding Ru360.

Two electrode voltage clamp (TEVC). TEVC was performed using a *Xenopus* oocyte system.[9] Briefly, stage V-VI oocytes were injected with 30 ng of cRNA encoding a human MCU-EMRE fusion protein, and incubated in 18 ℃ in an ND96 solution (96 mM NaCl, 2 mM KCl, 2 mM $CaCl_2$, 0.5 mM $MgCl_2$, 5 mM HEPES, pH 7.4-NaOH). Recordings were performed 2 days after cRNA injection. An Oocyte Clamp OC-725B system (Warner) was used to acquire signals, which were filtered at 1 kHz and sampled at 2 kHz. Digitization and voltage control were carried out using a Digidata-1322A/pClamp-10 system (Molecular Devices). In all experiments, oocytes were perfused with a Ca-20 solution (70 mM NaCl, 2 mM KCl, 0.5 mM $MgCl_2$, 20 mM $CaCl_2$, 5 mM HEPES, pH 7.4-NaOH). After establishing the voltage clamp, the oocyte was then treated with indicated compounds, dissolved in the Ca-20 solution, to inhibit the MCU.

3. CYTOTOXICITY AND CELLULAR UPTAKE STUDIES

Cytotoxicity Assay. HeLa or HEK293T cells were seeded in 96-well plates with ~2000 cells/well and incubated overnight. The following day, the culture media was removed, and cells were treated with media containing varying concentrations of the complex and incubated for 72 h. Following treatment, the cells were incubated in DMEM containing 1 mg/mL (4,5-dimethylthiazol-2-yl)-2,5-diephenyltetrazolium bromide (MTT) without FBS for 3 – 4 hours. Following incubation, the media was removed, and the purple formazan crystals were solubilized using 200 μL of an 8:1 DMSO/glycine buffer (pH 10) mixture. The absorbance at 570 nm of each well was measured using a BioTek Synergy HT plate reader. Results are reported as the average cell viability of 6 wells/concentration compared to untreated cells from three independent trials ± SD.

Mitochondrial Membrane Potential via JC-1 Assay. Approximately 1×10^5 HeLa or HEK293T cells were seeded in 35 mm glass-bottomed dishes and incubated overnight at 37 °C. On the next day, cells were treated with the desired metal complex (50 μM) and incubated for a further 24 h. The culture media was removed and replaced with fresh media containing 10 μM JC-1 dye and incubated at 37 °C in the dark for 30 min. The media was removed, and the cells were washed with 2 × 1 mL PBS before imaging. The cells were imaged in 1 mL PBS. Control dishes were handled identically to the treated cells except they were not treated with metal complex. For the positive control dishes, cells were treated with 50 μM carbonyl cyanide m-chlorophenyl hydrazine (CCCP) in PBS and the cells were imaged without removal of CCCP. The cells were imaged using a 488 nm laser excitation with a 400–545 nm green emission filter for the green monomer fluorescence and 575–700 nm red emission filter for the J-aggregate fluorescence. The cellular images were analyzed using ImageJ and the CTCF was used to compare cellular fluorescence. For each replicate, the average red/green fluorescence ratio was determined using at least 8 independent cells and was normalized to untreated control cells ($[red/green]_{control} = 1$). Data are reported as the average of three independent trials ± SD.

Cellular Uptake Assay. HeLa or HEK293T cells were grown to near confluence in 6-well plates. On the day of the experiment, the culture media was removed, and the cells were treated with fresh media containing 0 or 50 μM complex and incubated for 3 h at 37 °C. The culture media was then removed, and the adherent cells were washed with 3 × 1 mL of PBS and harvested with trypsin before being pelleted by centrifugation (800 × *g* for 10 min). The cell pellet was suspended in ice cold lysis buffer (1% w/v 3-[3-cholamidopropyl)dimethylammonio]-1-propanesulfonate), 5 mM EDTA, 50 mM tris(hydroxymethyl)aminomethane (Tris) and 100 mM NaCl; pH = 7.4). The suspension was vortexed for 30 s and incubated on ice for 45 min. The cell lysate was centrifuged to remove precipitated debris and the supernatant was transferred to a clean tube prior to analysis. The Co content of the lysate was determined using GFAAS and was normalized to the protein content of the sample, which was determined using the bicinconinic acid (BCA) assay kit following manufacturer instructions (ThermoFisher). Results are reported as the average mass ratio of Co to protein (pg/μg) in each sample ± SD ($n = 4 – 5$).

Mitochondrial Isolation Protocol. Mitochondrial isolation was performed using a protocol that is virtually identical to that previously reported by us.[1] Briefly, approximately 1×10^6 HeLa cells were seeded in 10 cm^2 culture dishes and allowed to adhere overnight. The following day, the cells were treated with 50 μM **3** in normal culture media for 3 h at 37 °C. Following treatment, the cells were washed with 3 × 3 mL room temperature PBS and harvested with trypsin. The cells were collected by centrifugation (800 × *g* for 10 min) and suspended in 500 μL of ice cold mitochondrial isolation buffer (pH 7.4) containing 200 mM mannitol, 68 mM sucrose, 50 mM piperazine-N,N′-bis(2-ethanesulfonic acid), 50 mM KCl, 5 mM EGTA, 2 mM $MgCl_2$, 1 mM dithiothreitol, and 1:500 v/v protease inhibitor cocktail. The cell suspension was then incubated on ice for 20 min before it was homogenized by 40 passes through a 25-guage needle using a 1 mL syringe. The homogenized suspension was centrifuged at 150 × *g* for 5 minutes. The supernatant was transferred to a clean tube and centrifuged for 10 min at 14,000 × *g* to pellet the mitochondrial fraction. The remaining solid from the first centrifuging step was lyophilized overnight before digestion in 300 μL of 70% HNO_3 (trace metal grade). The mitochondrial pellet was suspended in 300 μL distilled water and sonicated for 30 s on ice. The cobalt concentration of each fraction was determined by GFAAS and was normalized to the protein content of the sample using the BCA assay as described above. Samples that were measured by GFAAS were either diluted to < 2% HNO_3 or supplemented with fresh HNO3 to give the same concentration in each sample to account for possible matrix effects. Each replicate consisted of cells combined from three 10 cm^2 dishes. Results are reported as the mass ratio of total cobalt to protein (pg / μg) in each sample ± standard deviation of three independent trials.

4. DOCKING STUDIES

Docking studies were performed using the program GOLD.[10,11] The structure of each complex was optimized using density functional theory (DFT) using Gaussian 16 using the crystal structure (**1**,[12] **2**,[13] **3**,[14] **4**,[15] **5**,[16] **6**,[17] Ru265′[18]) as a starting geometry. The BP86 functional[19] was used for geometry optimization and frequency calculations in the gas phase. The metal centers were handled using a relativistic core potential (ECP10MDF for Co[20] and ECP28MWB for Ru[21]) and the related basis sets, while the light atoms (C, H, N, O) were treated with the 6-31G(d,p) basis set. All complexes were optimized in the singlet state and the optimized coordinates are included as part of the SI. The HERMES visualizer was used to further prepare the metal complex and protein for docking. The docking cavity of the tetrameric MCU (PDB 6O5B) was defined as the centroid of the four aspartate residues in the DXXE region of MCU pore and included all residues within 10 Å of this point. Default values for all other parameters were used and the complexes were subjected to 100 genetic algorithm runs using the piecewise linear potential ChemPLP[22] scoring function to evaluate the docked results.

5. SUPPLEMENTARY FIGURES AND TABLES

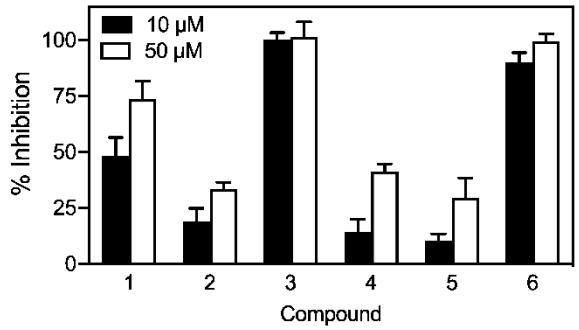

Figure S1. Quantification of MCU-inhibitory activity of the Co^{3+} complexes as reflected by mt-Ca^{2+} uptake rate in permeabilized HeLa cells (5×10^6 cells mL^{-1}) at 10 and 50 μM. Data are reported as the mean % inhibition compared to control cells ± 1 standard deviation (SD, $n = 3$).

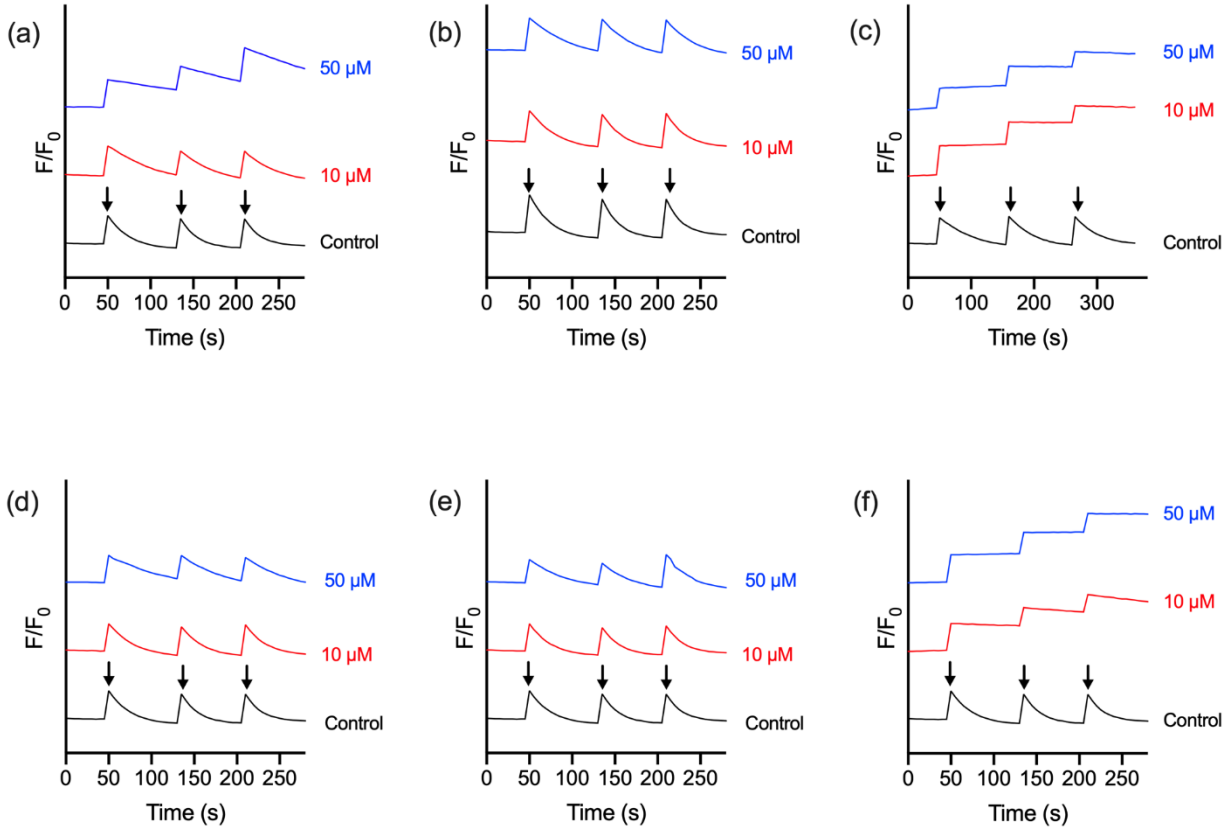

Figure S2. Representative traces of extramitochondrial Ca^{2+} clearance in permeabilized HeLa cells (5×10^6 cells mL^{-1}) treated with either 10 μM or 50 μM of (a) **1**, (b) **2**, (c) **3**, (d) **4**, (e) **5**, or (f) **6**. Arrows indicate addition of 10 μM Ca^{2+}. Each complex was tested in triplicate using independently prepared cell suspensions and complex stock solutions.

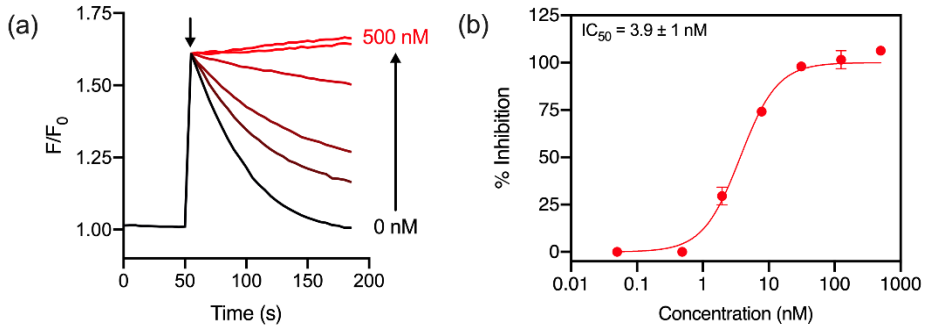

Figure S3. (a) Representative traces of extramitochondrial Ca^{2+} clearance in permeabilized HeLa cells (5×10^6 cells mL^{-1}) treated with varying concentrations of Ru265 after addition of 10 µM Ca^{2+}. The arrow indicates time of addition. (b) Dose-response curve for mt-Ca^{2+} uptake inhibition by Ru265. Data are represented as mean ± SD (n = 3 – 4).

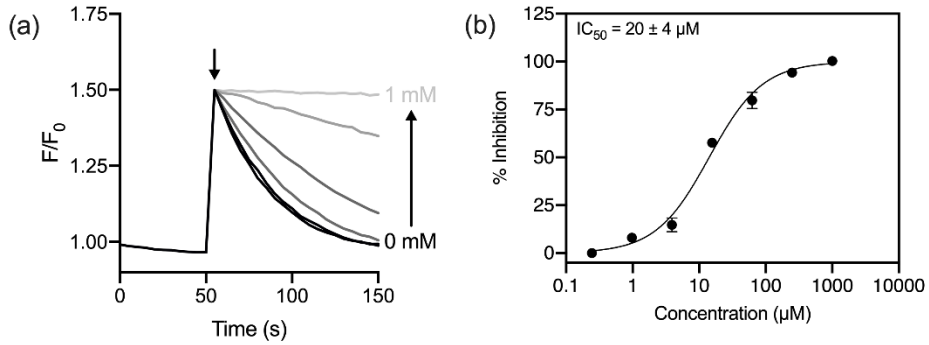

Figure S4. (a) Representative traces of extramitochondrial Ca^{2+} clearance after addition of 10 µM Ca^{2+} in permeabilized HeLa cells (5×10^6 cells mL^{-1}) treated with varying concentrations of **1**. The arrow indicates time of Ca^{2+} addition. (b) Dose-response curve for mt-Ca^{2+} uptake inhibition by **1**. Data are represented as mean ± SD (n = 3 – 4).

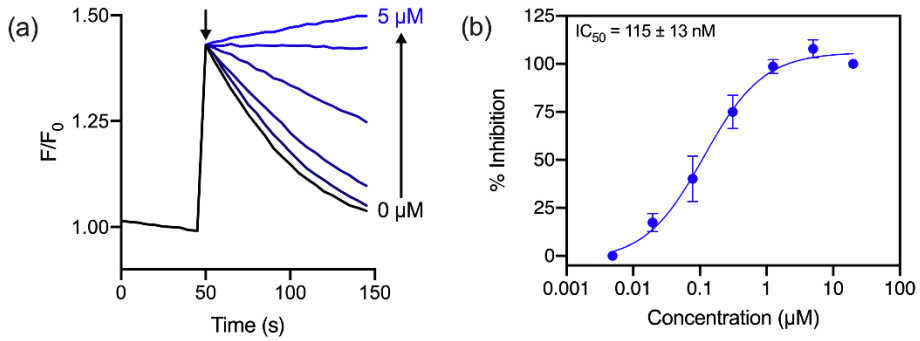

Figure S5. (a) Representative traces of extramitochondrial Ca^{2+} clearance after addition of 10 μM Ca^{2+} in permeabilized HeLa cells (5×10^6 cells mL^{-1}) treated with varying concentrations of **3**. The arrow indicates time of Ca^{2+} addition. (b) Dose-response curve for mt-Ca^{2+} uptake inhibition by **3**. Data are represented as mean ± SD (n = 3 – 4).

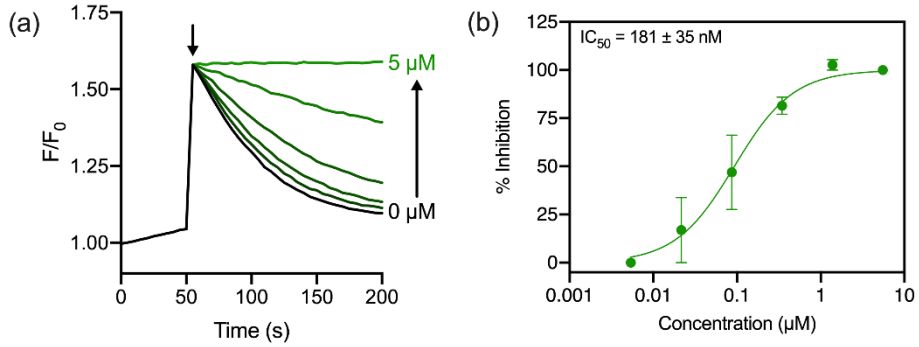

Figure S6. (a) Representative traces of extramitochondrial Ca^{2+} clearance after addition of 10 μM Ca^{2+} in permeabilized HeLa cells (5×10^6 cells mL^{-1}) treated with varying concentrations of **6**. The arrow indicates time of Ca^{2+} addition. (b) Dose-response curve for mt-Ca^{2+} uptake inhibition by **6**. Data are represented as mean ± SD (n = 3 – 4).

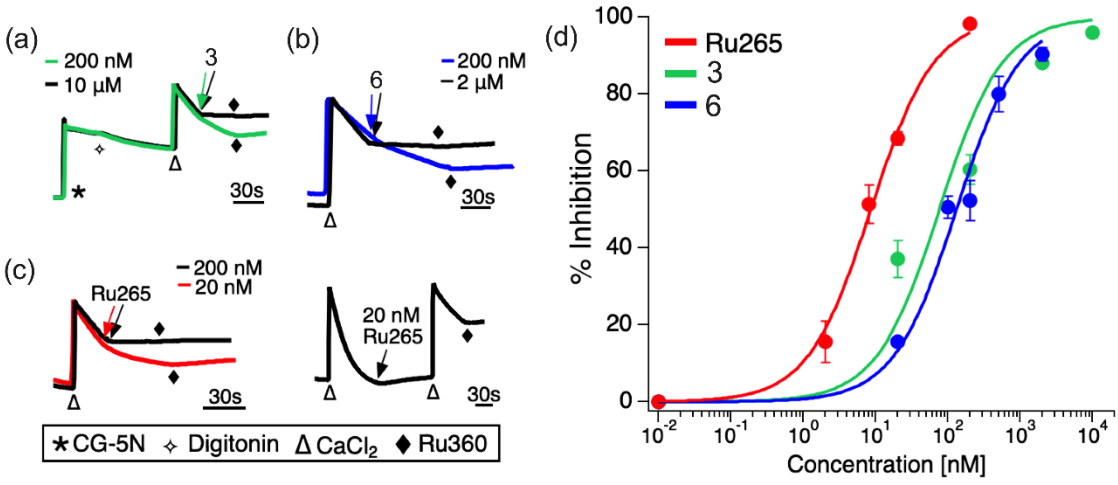

Figure S7. Representative traces of extramitochondrial Ca^{2+} clearance after addition of 15 μM Ca^{2+} in permeabilized HEK293 cells (10^7 cells mL^{-1}) treated with different concentrations of (a) **3**, (b) **6**, or (c) Ru265. (d) Dose-response curves for mt-Ca^{2+} uptake inhibition by **3**, **6**, and Ru265. Data are represented as mean ± S.E.M. (n = 3 – 5).

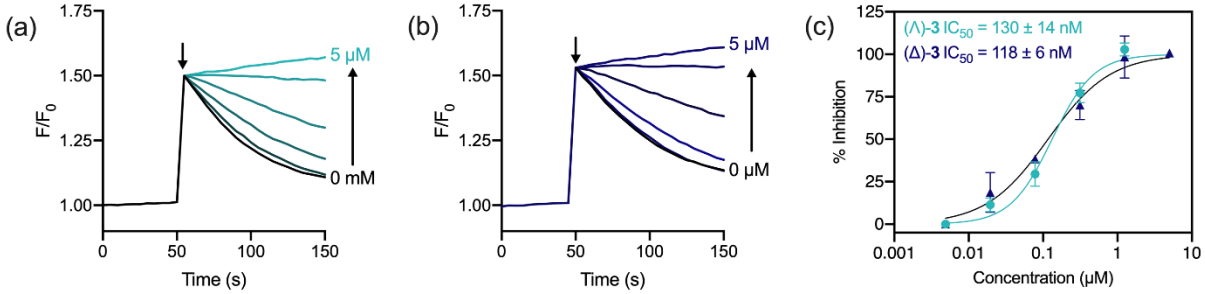

Figure S8. Representative traces of extramitochondrial Ca^{2+} clearance after addition of 10 μM Ca^{2+} in permeabilized HeLa cells (5×10^6 cells mL^{-1}) treated with varying concentrations of (a) **3a** or (b) **3b**. The arrow indicates time of Ca^{2+} addition. (c) Dose-response curves for mt-Ca^{2+} uptake inhibition by **3a** and **3b**. Data are represented as mean ± SD (n = 3 – 4).

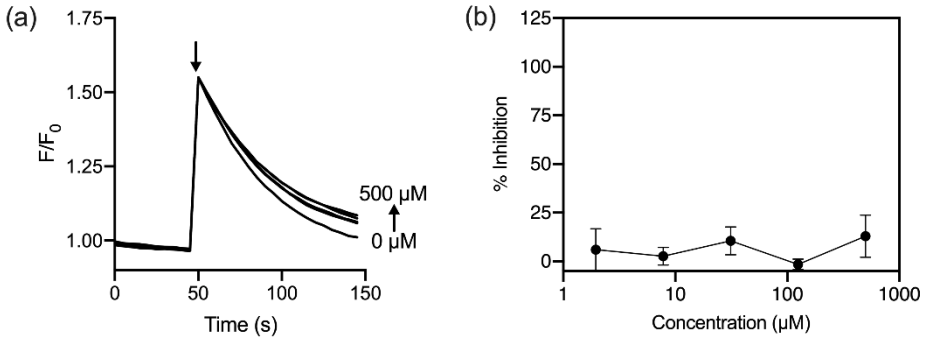

Figure S9. (a) Representative traces of extramitochondrial Ca^{2+} clearance after addition of 10 μM Ca^{2+} in permeabilized HeLa cells (5×10^6 cells mL^{-1}) treated with 10 μM ethylenediamine (en). The arrow indicates time of Ca^{2+} addition. (b) Dose-response plot for mt-Ca^{2+} uptake in the presence of en. Data are represented as mean ± SD (n = 3).

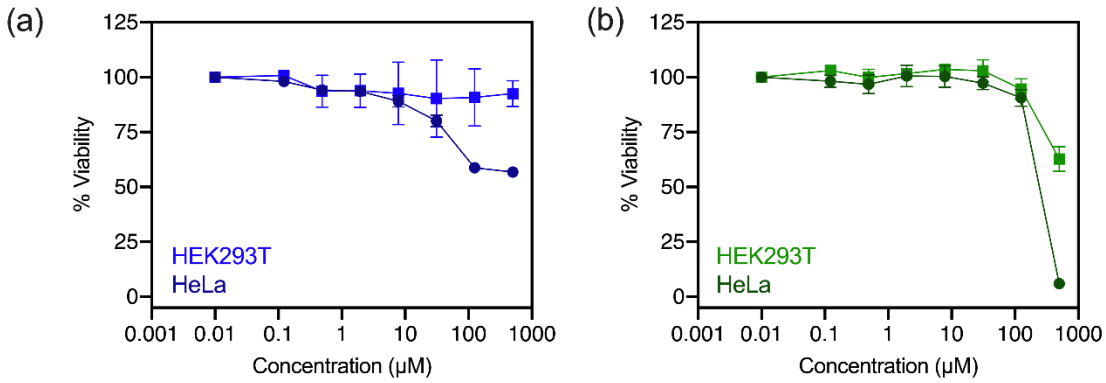

Figure S10. Cell viability curves of HeLa and HEK293T cells treated with varying concentrations of (a) **3** and (b) **6** for 72 h. Results are represented as mean ± SD of three independent trials with 6 wells/concentration.

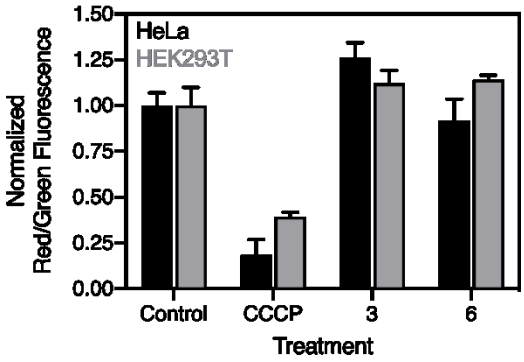

Figure S11. Normalized red/green fluorescence intensity of HeLa and HEK293T cells after treatment with the corresponding compounds and 10 µM JC-1 dye. See Figure S12-S13 for representative confocal fluorescence microscopy images.

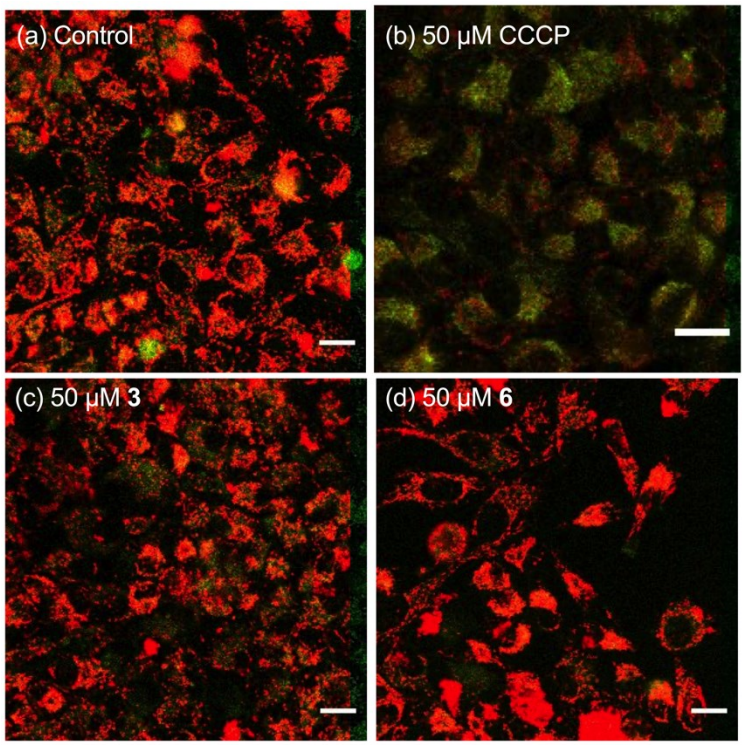

Figure S12. Representative confocal fluorescence microscopy images of HeLa cells treated with JC-1 dye and (a) no compound (b) 50 µM CCCP for 2 min, (c) 50 µM **3** for 24 h, and (d) 50 µM **6** for 24 h. The scale bar represents 20 µm.

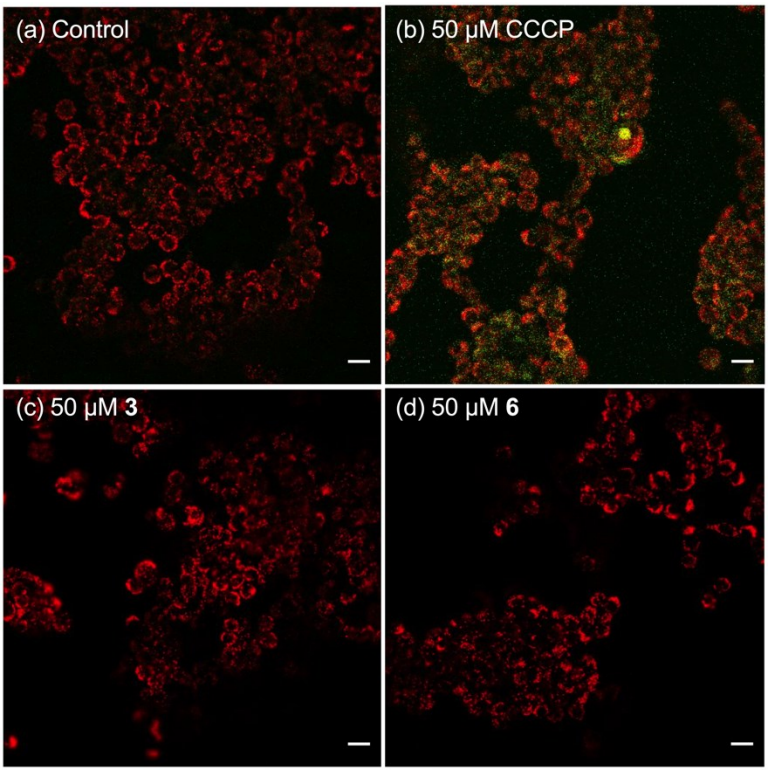

Figure S13. Representative confocal fluorescence microscopy images of HEK293T cells treated with JC-1 dye and (a) no compound, (b) 50 μM CCCP for 2 min, (c) 50 μM **3** for 24 h, and (d) 50 μM **6** for 24 h. The scale bar represents 20 μm.

Figure S14. Cellular accumulation of Ru265, **3**, and **6** in HeLa and HEK293T cells treated with 50 μM complex for 3 h in DMEM supplemented with 10% FBS. Data are represented as mean ± SD (n = 3).

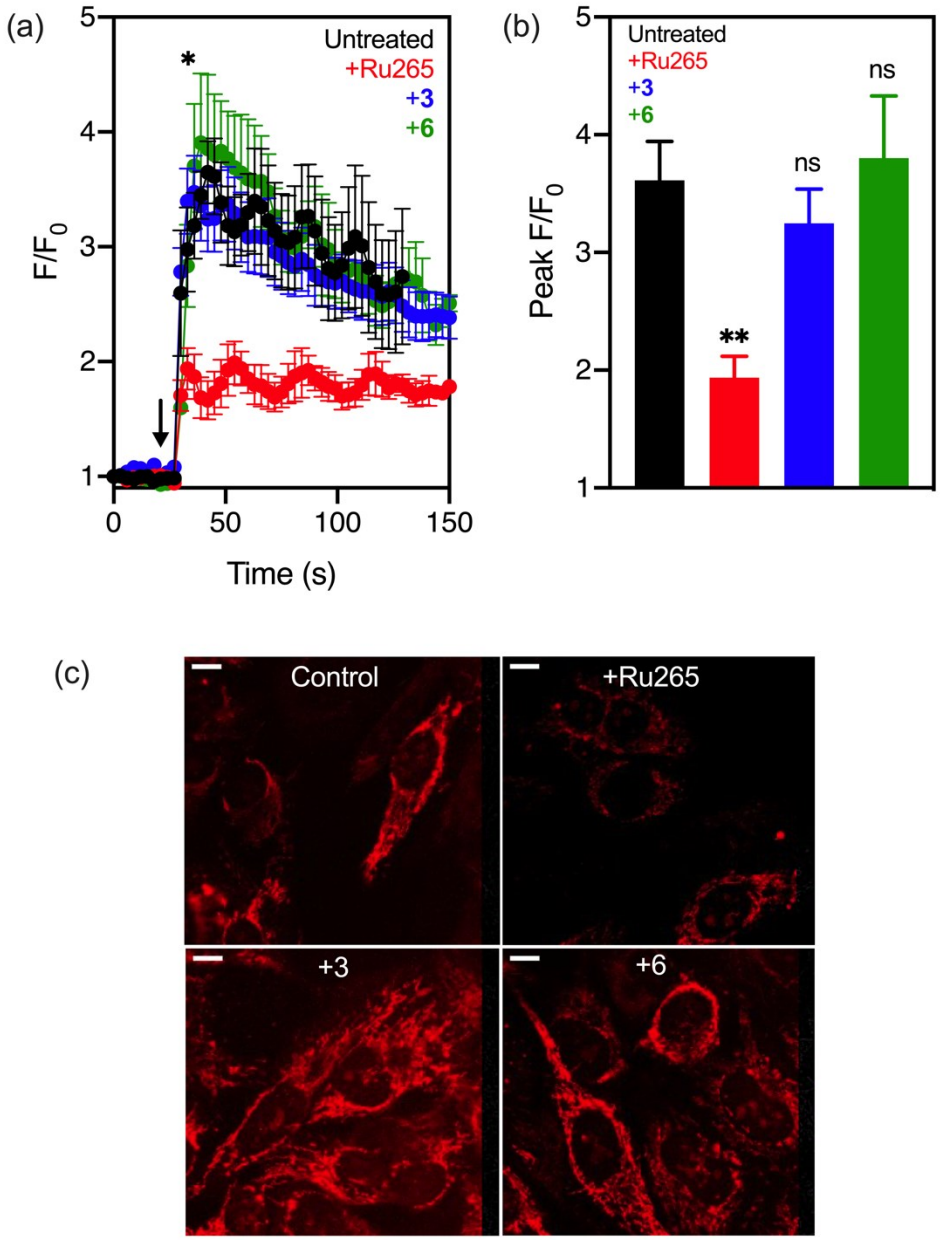

Figure S15. (a) Representative mt-Ca^{2+} accumulation after addition of 100 μM histamine in HeLa cells pretreated with 0 or 50 μM of Ru265, **3**, or **6** for 1 h and then loaded with 2 μM Rhod2AM. The arrow indicates time of histamine addition. (b) Quantification of peak F/F_0 at the point indicated by the star in panel a. (c) Representative fluorescence microscopy images of HeLa cells treated as described above at the point labeled by * in panel a. The scale bar represents 10 μm. Data are represented as mean F/F_0 of at least four cells ± SD from two independent biological replicates. **p<0.01 *vs* control, ns = not significant.

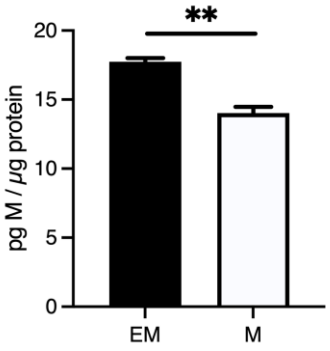

Figure S16. Comparison of the cobalt concentration in the extramitochondrial (EM) and mitochondrial (M) fraction of HeLa cells treated with compound **3**. The cells were treated with 50 μM complex for 3 h at 30 °C with no recovery in drug free medium. Cobalt concentration was normalized to protein content, which was determined using the BCA assay. Data are mean of three trials ± standard devation. $n = 3$, **$p<0.01$.

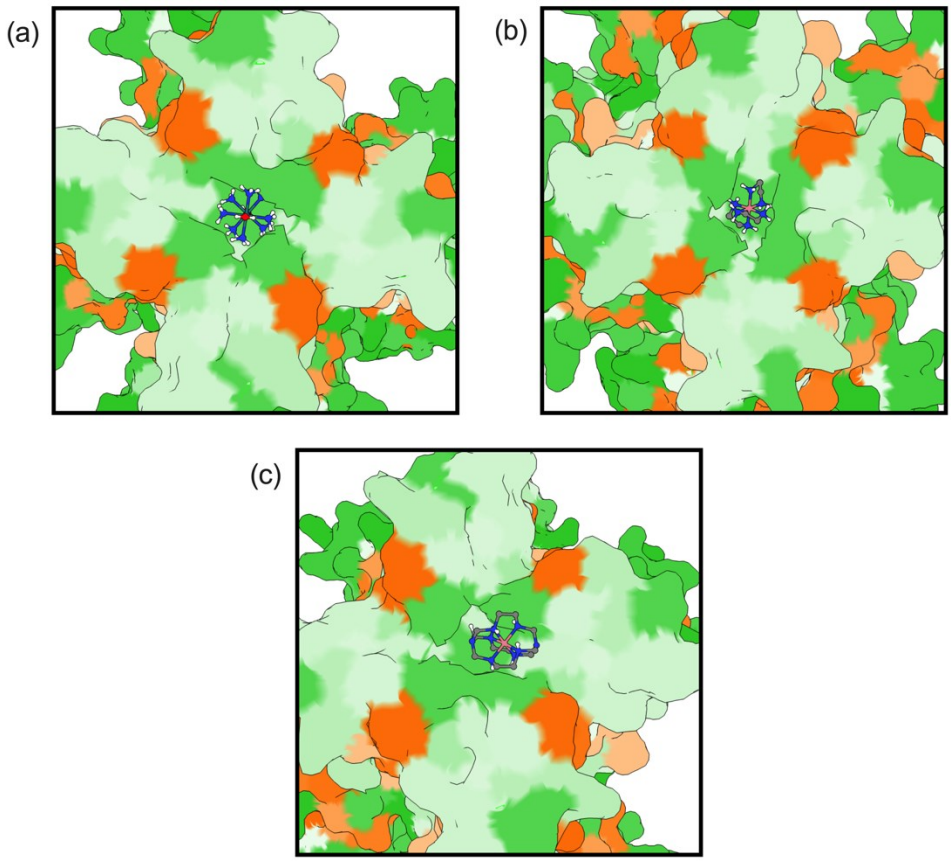

Figure S17. Top-down view of (a) Ru265, (b) **3**, and (c) **6** docked into the human MCU (PBD 6O5B). The surface is colored by amino acid hydrophobicity (lime green = hydrophilic, orange = hydrophobic).

Table S1. Comparison of the relative docking scores of the metal complexes docked into the DIME region of the human MCU (PDB 6O5B).

Complex	ChemPLP Score
Ru265	51.15
1	45.75
2	46.97
3	33.59
4	25.24
5	19.61
6	28.13

6. REFERENCES

(1) Woods, J. J.; Nemani, N.; Shanmughapriya, S.; Kumar, A.; Zhang, M.; Nathan, S. R.; Thomas, M.; Carvalho, E.; Ramachandran, K.; Srikantan, S.; Stathopulos, P. B.; Wilson, J. J.; Madesh, M. *ACS Cent. Sci.* **2019**, *5*, 153–166.
(2) Nathan, S. R.; Pino, N. W.; Arduino, D. M.; Perocchi, F.; MacMillan, S. N.; Wilson, J. J. *Inorg. Chem.* **2017**, *56*, 3123–3126.
(3) Schlesssinger, G. G.; Schlessinger, G. G.; Britton, D.; Rhodes, T.; Ng, E. *Inorg. Synth.* **1967**, *9*, 160–163.
(4) Broomhead, J. A.; Dwyer, F. P.; Hogarth, J. W. *J. Chem. Educ.* **1960**, *53*, 667.
(5) Broomhead, J. A.; Dwyer, F. P.; Hogarth, J. W.; Sievers, R. E. *Inorg Synth* **1960**, *6*, 183–186.
(6) Keene, F. R.; Searle, G. H. *Inorg. Chem.* **1972**, *11*, 148–156.
(7) Wieghardt, K.; Schmidt, W.; Herrmann, W.; Kueppers, H. J. *Inorg. Chem.* **1983**, *22*, 2953–2956.
(8) Harrowfield, J. M.; Herlt, A. J.; Sargeson, A. M.; Donno, T. Del. *Inorg. Synth.* **1980**, *20*, 85–86.
(9) Tsai, C. W.; Tsai, M. F. *J. Gen. Physiol.* **2018**, *150*, 1035–1043.
(10) Jones, G.; Willett, P.; Glen, R. C.; Leach, A. R.; Taylor, R. *J. Mol. Biol.* **1997**, *267*, 727–748.
(11) Cole, J. C.; Nissink, J. W. M.; Taylor, R. In *Virtual Screening in Drug Discovery*; Soichet, B., Alvarez, J., Eds.; Taylor and Francis CRC Press: Boca Raton, FL, 2005.
(12) Bernhardt, E.; Brauer, D. J.; Finze, M.; Willner, H. *Angew. Chem. Int. Ed.* **2006**, *45*, 6383–6386.
(13) Stanko, J. A.; Paul, I. C. *Inorg. Chem.* **1967**, *6*, 486–490.
(14) Nakatsu, K.; Saito, Y.; Kuroya, H. *Bull. Chem. Soc. Jpn.* **1956**, *29*, 428–434.
(15) Tang, C.; Wang, F.; Jiang, W.; Zhang, Y.; Jia, D. *Inorg. Chem.* **2013**, *52*, 10860–10868.
(16) Kueppers, H. J.; Neves, A.; Pomp, C.; Ventur, D.; Wieghardt, K.; Nuber, B.; Weiss, J. *Inorg. Chem.* **1986**, *25*, 2400–2408.
(17) Ribeiro, S.; Cunha-Silva, L.; Balula, S. S.; Gago, S. *New J. Chem.* **2014**, *38*, 2500–2507.
(18) Woods, J. J.; Lovett, J.; Lai, B.; Harris, H. H.; Wilson, J. J. *Angew. Chem. Int. Ed.* **2020**, *59*, 6482–6491.
(19) Becke, A. D. *Phys. Rev. A* **1988**, *38*, 3098–3100.
(20) Dolg, M.; Wedig, U.; Stoll, H.; Preuss, H. *J. Chem. Phys.* **1986**, *86*, 866–872.
(21) Peterson, K. A.; Figgen, D.; Dolg, M.; Stoll, H. *J. Chem. Phys.* **2007**, *126*, 124101.
(22) Korb, O.; Stützle, T.; Exner, T. E. *J. Chem. Inf. Model.* **2009**, *49*, 84–96.